Overview of JET Results in Support of the ITER Physics Basis

The JET Team* (prepared by C. Gormezano[1)])

JET Joint Undertaking, Abingdon, United Kingdom

[1)]present address: Associazone EURATOM-ENEA sulla Fusione, Frascati, Italy

e-mail contact of main author: gormezano@frascati.enea.it

Abstract. The JET experimental campaign has focused on studies in support of the ITER physics basis. An overview of the results obtained is given both for the reference ITER scenario, the ELMy H-mode, and for advanced scenarios which in JET are based on Internal Transport Barriers. JET studies for the ELMy H-mode have been instrumental for the definition of ITER-FEAT. Positive elongation and current scaling in the ITER scaling law have been confirmed, but the observed density scaling fits better a two term (core and edge) model. Significant progress in neo-classical tearing mode limits has been made showing that ITER operation seems to be optimised. Effective helium pumping and divertor enrichment is found to be well within ITER requirements. Target asymmetries and H-isotope retention are well simulated by modelling codes taking into account drift flows in the scrape-off plasmas. Striking improvements in fuelling effectiveness have been found with the new high field pellet launch facility. Good progress has been made on scenarios for achieving good confinement at high densities, both with RI modes and with high field side pellets. Significant development of advanced scenarios in view of their application to ITER has been achieved. Integrated advanced scenarios are in good progress with edge pressure control (impurity radiation). An access domain has been explored showing in particular that the power threshold increases with magnetic field but can be significantly reduced when Lower Hybrid current drive is used to produce target plasma with negative shear. The role of ion pressure peaking on MHD has been well documented. Lack of sufficient additional heating power and interaction with the septum at high beta prevents assessment of beta limits (steady plasmas achieved with β_N up to 2.6). Plasmas with non-inductive current ($I_{NI}/Ip=60\%$), well aligned with plasma current, high beta and good confinement have also been obtained.

1. Introduction

The main results from the JET DT campaign were presented at the last IAEA conference together with the preliminary results obtained with the new JET divertor, the high closure Gas Box divertor (MKIIGB). In 1999, a high field side pellet injector was installed, mainly using remote handling tools. It is to be noted that JET was operated for more than 2 years at full specifications, including tritium, without human intervention in the vacuum vessel. Among diagnostic improvements, the Motional Stark Effect diagnostic, allowing the plasma current profile to be measured, has been made fully operational. The recent JET experimental campaign has been mostly devoted to studies in support of the ITER physics basis, especially in view of the redefinition of the ITER design leading to ITER-FEAT. The two main scenarios considered for ITER have been studied. The reference ITER scenario is the ELMy H-mode scenario, which is already well documented. Physics studies have focused on improving understanding and optimisation of critical parameters: divertor physics, fuelling studies, MHD limits and confinement issues. In JET, advanced scenarios are based on plasmas with Internal Transport

---

* See Appendix

Barriers (ITB), this scenario being in a much earlier stage of development. Corresponding studies have focused on the extrapolability of this scenario: MHD stability, domain of existence and fuelling, and to the development of integrated scenarios: steady plasmas at high beta, beta limits and high non-inductive current drive fraction.

2. ELMy H-mode Studies

2.1. Divertor Studies

Divertor tile thermocouples have been used to measure the target energy deposition and give a reasonable power balance. A substantial part of the ELM energy is deposited on the divertor targets rather than on the vessel walls. A large asymmetry is observed, two or three times as much energy going to the outer strike target than to the inner, which does not change significantly with ELM frequency, from 0 to 250 kHz. Power profiles deduced from pulse by pulse shifting of typical ELMy H mode plasmas show a narrow peak carrying out 50% of the total divertor power (Fig.1), which is 2-3 mm in width, a feature that is not explained by conventional models [1]. This feature has been confirmed using H-modes with the X point resting on the septum, the high flux expansion associated with these plasmas meaning that the septum only intercepts flux surfaces out to 2mm with 50% of the energy being deposited there.

Flows in the scrape-off layer (SOL) play an important role as exemplified in Fig.2 showing that when the magnetic configuration is varied from normal to reversed ∇B, the SOL flow reverses from the inside to the outside. Understanding the role of drifts is indeed important for ITER. Observed asymmetries are well modelled with the EDGE2D code when various drifts are taken into account [2]. The flow pattern consists mainly of the ion Pfirsh-Schluter flow and of the return parallel flow created by the poloidal E_rxB drift. ∇B and centrifugal drifts cause the largest asymmetries consistent with the effect of the j_rxB forces.

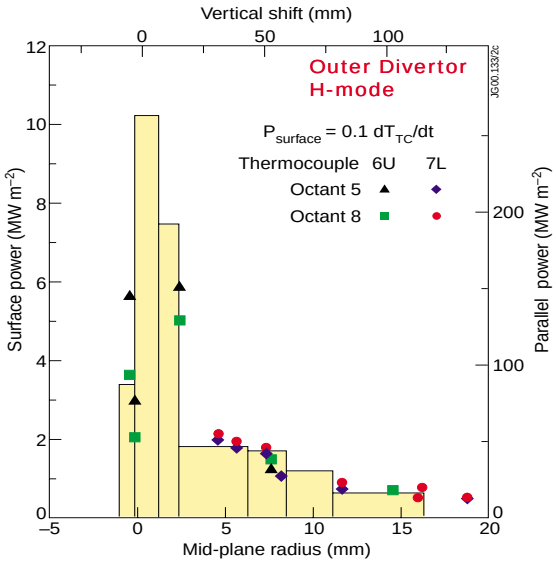

FIG.1. Power profiles for the outer divertor for 12 MW H-mode plasmas without gas fuelling.

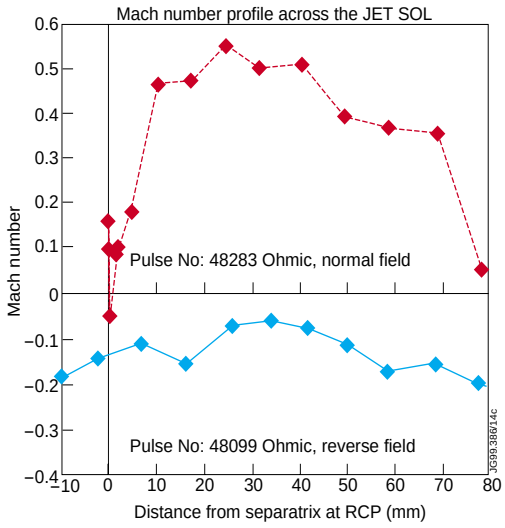

FIG.2. Mach number profiles across the SOL measured with the reciprocating probe with normal and reversed ∇B discharges.

Deposition and H-isotope retention has also been found to be highly asymmetric with deposition predominantly in the inner divertor. The majority of the tritium retained in JET after the DT campaign is in the form of flakes deposited on the water-cooled louvres, which are shadowed from the plasma. This asymmetry is consistent with the outboard to inboard flow that occurs in normal JET operating conditions. If such a drift is included in the DIVIMP model **[**3], the deposition asymmetry can be well reproduced assuming higher sputtering values than those usually taken are used and that some redeposition processes are taken into account.

Helium exhaust in a reactor is a determining factor in fusion efficiency and is determined by a combination of intrinsic transport of helium and of enrichment and helium compression in the divertor. Specific experiments on helium transport and exhaust have been made by using argon frosting techniques which allow an helium pumping of about 75 % of the deuterium pumping to be achieved for several pulses (typically 3) following a fresh layer of argon on the cryo-panels **[**4**]**. Studies have been mainly performed in ELMy H-mode plasmas similar to those considered for ITER. As shown in Fig. 3, in optimum pumping conditions, a ratio for $\tau^*_P(He)/\tau_E$ of 7.6 has been found ($\tau_P^*=\tau_P/(1-R_{eff})$, R_{eff} being the He recycling coefficient), well below the required

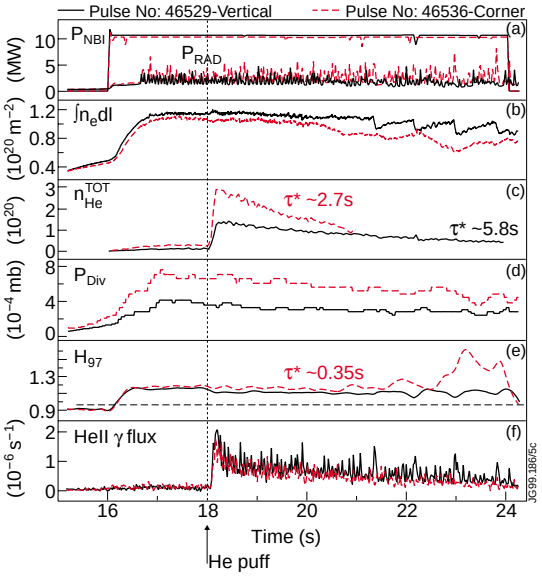

FIG.3. Comparison of helium concentration decay (c)and (f) for two ELMy H-modes (1.9MA/2T) at constant input power.

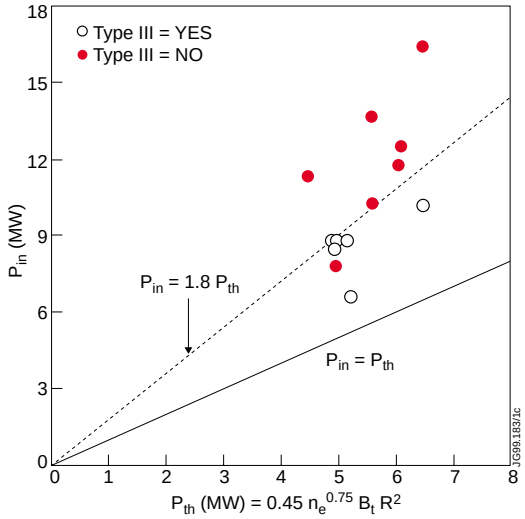

FIG.4. Injected power versus H-mode power threshold for steady type I ELMs (from scans in Ip and B).

maximum value of 15 considered for ITER. As well, the helium enrichment in the divertor has been found to be $0.5<\eta(He)<1.0$, well above the value of 0.2 required for ITER. These results are encouraging in showing that helium transport and exhaust might not be a problem for the ITER reference scenario.

It is important on a given experiment, such as ITER, to be able to reach high steady confinement regimes, which is generally achieved with a type I ELM H-mode. But, the power required to maintain such a regime is about 1.8 times the threshold power for H-mode **(**Fig. 4**)**, with an irreproducibility of about 20% probably indicative of vessel conditioning effects [5]. It is to be noted that increasing triangularity decreases the power threshold and that Type I ELMs revert to

type III ELMs in the MKIIGB divertor, while they were reverting to L-mode in the MKII divertor.

Among the physical parameters that influence the width of the edge transport barrier, the influence of fast particles (effect of ion larmor radius) is an important issue for a burning plasma experiment such as ITER. A comparison has been made between ELMy H-modes with a variable proportion of NBI, producing fast ions mainly at the edge and of ICRH which produces a large population of fast ions mainly in the core [6]. As shown in Fig 5, Elms of similar frequency are produced in NBI and ICRH dominated plasmas in conditions where gas fuelling and edge densities were carefully matched. Although the edge fast particle concentration varies from 4% to 0.4% in this scan, both edge and core parameters do not vary significantly, core confinement of ICRH plasmas being slightly higher due to a more central heat deposition. In these regimes, fast ions do not play a dominant role for the edge stabilisation between ELMs.

2.2. Fuelling Studies

The installation of a pellet launcher on the high field side (HFS) of JET was motivated by the more effective fuelling which can be anticipated due to the ExB acceleration of the cold ablatant cloud in the direction of increasing major radius as already observed in other experiments (ASDEX-U, DIII-D). Penetration of the pellet is weakly dependent upon the speed of the pellet and decreases strongly with Te. In contrast, the net radial outward displacement is proportional

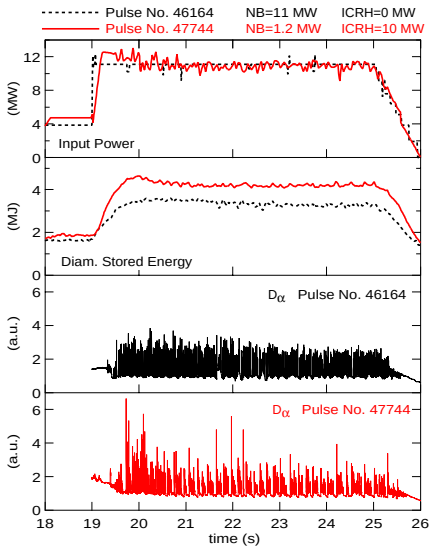

FIG.5.Divertor α emission for ELMy H-mode with variable NBI and ICRH power levels. All discharges are both fuelled with D + 5%H at a constant rate of 1x10^{22}s^{-1}.

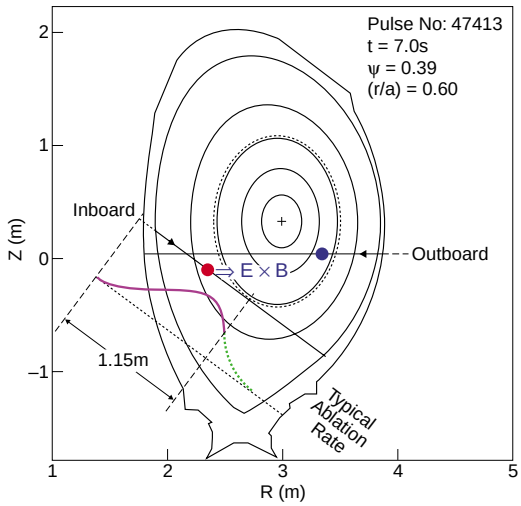

FIG.6. Geometry of outboard and inboard pellet launch trajectories. Typical ablation profile and schematic indication of ExB drift beyond ablation. zone are shown for inboard launch.

to the temperature of the ablatant and the duration of the acceleration time, i.e. the time necessary to short out the polarisation field. The H-mode edge temperature is high which privilege the ExB acceleration but is detrimental for ablation. This allows core fuelling in an H-mode to be achieved. As can be seen in Fig 6, the geometry of the pellet centrifuge, which can inject 4mm pellets up to 10 Hz either on the outboard or the inboard side is optimised for good

penetration in H-mode [7]. Fuelling efficiencies have been measured in L-mode plasmas showing that indeed some deposition occurs beyond the tangency radius. For outboard fuelling, the change in electron density profile aligns spatially closely to the predicted ablation profile from the Neutral Gas Shielding (NGS) model [8]. The inboard launch unambiguously fuels the core region beyond the zone of ablation, consistent with the effects of the ExB drift. The contrast

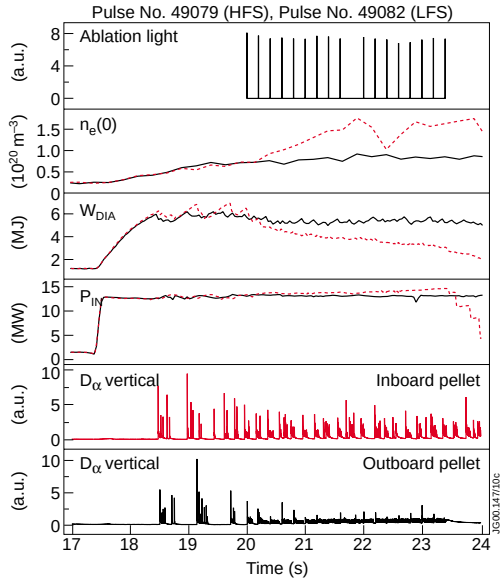

FIG.7. Comparison of HFS and LFS pellet fuelling of ELMy H-mode plasmas.

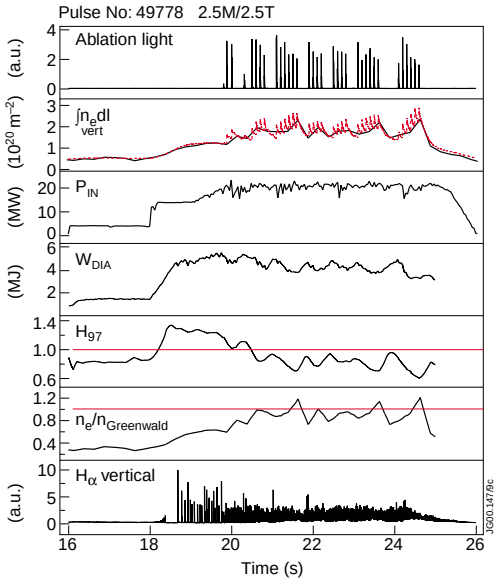

FIG.8. Optimisation of the HFS pellet sequence of an ELMy H-mode.

between HFS and low field side (LFS) launch is more dramatic for H-mode plasmas. Outboard pellets produce virtually no fuelling. As shown in Fig.7, a doubling of central density together with a peaking of the density profile is obtained, to the expense of a decrease in energy confinement attributed to a degradation of edge pedestal. HFS pellets allows densities much higher than the Greenwald density limit (n_G) to be achieved, up to n/n_G=1.6, but with H_{97}=0.5.It is possible to optimise the sequence of HFS pellets to increase confinement at high density [9, 10]. In effect, the pedestal parameters quickly recover after successive pellets while the plasma core density decays on a longer diffusion time scale comparable to the energy confinement time. Therefore, interrupting the pellet sequence allows a partial recovery of the energy content before the density decays fully. As shown in Fig.8, it is possible with this technique to maintain a good confinement with density in the range of the Greenwald density limit. Plasmas with good confinement corresponding to H_{97} of 0.9 have been achieved for n/n_G=0.85 in this way. Such a technique of pellet sequencing is very promising for application to ITER and needs to be further optimised

2.3. MHD Stability

Neo-classical tearing modes (NTM), which are triggered by other MHD events, usually sawteeth, can limit the plasma pressure well below ideal MHD beta limits and provide an upper limit to achievable fusion power. NTMs can cause a local flattening of the electron temperature around the q=3/2 or 5/2 magnetic surfaces in a pattern typical of a magnetic island. An

exploration of the dependence of the main plasma parameters around values of interest for ITER has been performed, especially in studying effects which might improve performance such as shaping and plasma current. Raising the plasma current, i.e. lowering q_{95} results in improved confinement and thus could increase the ITER operating domain. The critical beta for the onset of NTMs is plotted q_{95}, in Fig.9 **[**11**]**. The data are from a scan in plasma current but also shown are the data corrected for magnetic field and density variations using standard scaling laws. For q_{95} >3, there is a small decrease of the β_{Ncrit}, the NTMs reducing the confinement by 5 to 20%, while for lower values of q_{95} there is a sharp fall off in accessible β_{Ncrit}. In the low q domain, NTMs can eventually lead to disruptions and it appears not possible to make use of improvement in confinement associated with higher plasma current. Present ITER parameters (q_{95}~3.3) are set in the safer range.

Increasing plasma shape is also a way to improve plasma performance. Variation of both elongation and triangularity appears to not affect significantly beta threshold for NTM onset. It is important to understand the underlying physics of the NTM in order to separate elongation from triangularity effects and to support extrapolation for ITER. Analysis is based on the modified

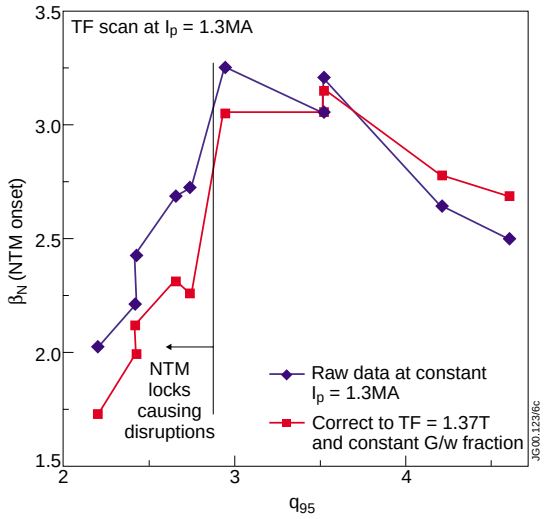

FIG.9. Change in β_N required for NTM onset with q_{95}; raw data and corrected for magnetic field and Greenwald density fraction variation

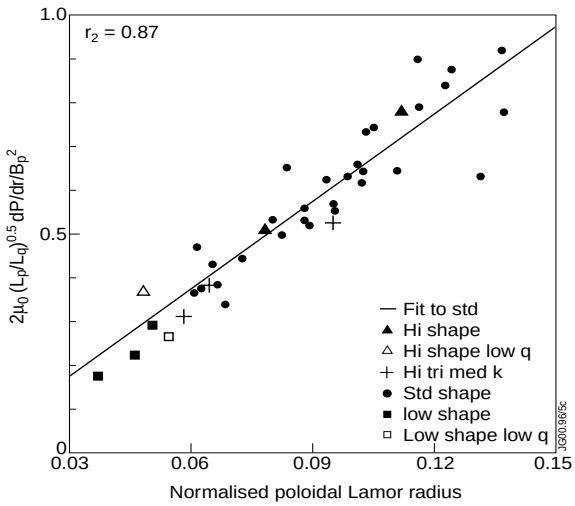

FIG.10. β_N threshold data for standard shape pulses using local variables. MKIIA and Gas Box data fit on the same regression line.

Rutherford equation for the growth rate of an island which is used for the NTM stability equation [11]. Data have been analysed in terms of physics parameters: tearing stability parameter, bootstrap current, ion polarisation current and possibly additional transport effects in the island. While there is a substantial scatter of data in a plot with β_N versus the normalised larmor radius, ρ^*, correlation and scatter are substantially improved when local parameters are used as shown in Fig.10. Local parameters include the scale lengths for safety factor, Lq, and for pressure gradients, Lp. The normalised poloidal larmor radius is indicative of the ion polarisation current that can dynamically screen the island. A more conclusive analysis is complicated by various effects that act in opposite way such as NTM seeding and shielding from the ion polarisation current. In effect recent studies indicate that triangularity is stabilising while elongation is destabilising [12]. Firmer conclusions require operation at lower ρ^* in order to

enter in a parameter space in which seed sizes are predicted to fall, raising thresholds as anticipated for ITER operation.

2.4. Confinement of ELMy H-modes

Confinement issues for ITER include the optimisation of shaping at plasma densities close to the Greenwald density limit. Configurations with large differences in elongation and also triangularity have been developed at ITER s request in view of the new ITER-FEAT design. In particular, elongation is a parameter which can improve confinement as shown in the IPB98(y,2) scaling law which is the reference for ITER:

$$\tau = 0.0562 x\, P^{-0.69} B^{0.15} I^{0.93} K_a^{0.78} n^{0.41} a^{0.58} R^{1.39} M^{0.19}$$

Three configurations were developed: the low elongation, low triangularity configuration corresponding to: κ=1.53 and δ=0.21, the high elongation, low triangularity configuration to κ=1.9 and δ=0.23 and the high elongation, high triangularity to κ=1.95 and δ=0.35. For each configuration, the minor radius and q_{95} were maintained respectively at 0.85m and 3.3. A gas scan was performed in ELMy H-mode plasmas with Ip=1.8 MA and q_{95} = 3.3. To assess the effect of shaping, elongation and confinement loss at high density, confinement is normalised to injected power, magnetic field, plasma current and major radius as given in terms of the IBP98 scaling law. As shown in Fig.11, energy confinement increases with elongation and a regression analysis gives $\tau \sim K_a^{0.8-0.3}$, in line with the wider JET database [13]. Further scenarios to study the effect of current and magnetic field were also developed and their positive scaling was found to be in line with the ITER scaling law.

The effect of triangularity was found to be quite small in contrast with earlier results from JET and ASDEX-U [14], but optimisation of the scenario such as using different gas fuelling was not done. Relative effects of upper against lower triangularity might also plays a role. Nevertheless,

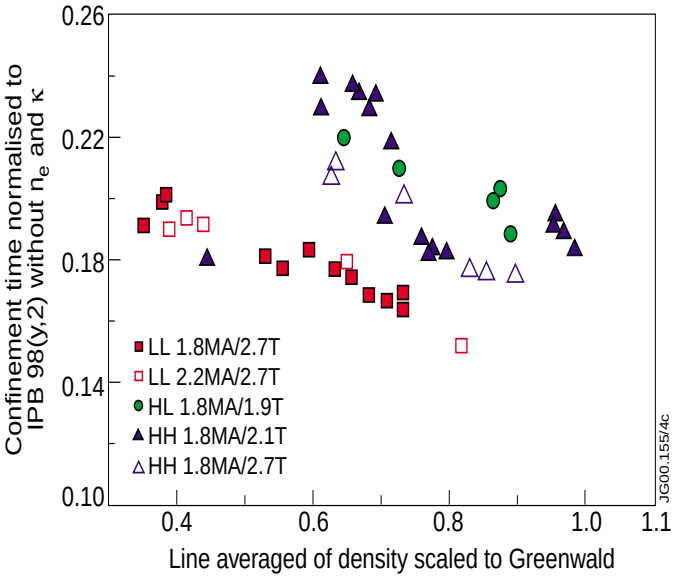

FIG.11. Confinement time normalised for power, current and field versus density for various shapings. The HH point at low density has a lower confinement due to the onset of NTMs.

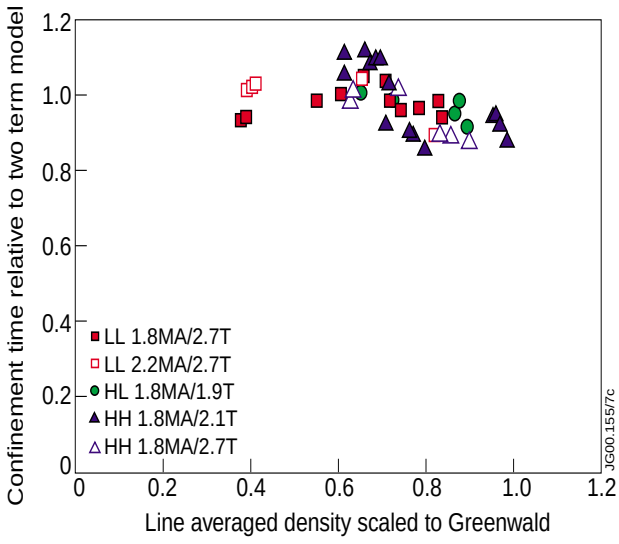

FIG.12. Confinement versus density using data normalised with a two term scaling law.

in all scenarios there is a fall in confinement as the density is increased towards the Greenwald limit. This is believed to be due to pedestal degradation. A two term scaling law has been developed [13] with separate terms reflecting the core confinement, taken as gyro-bohm, and the pedestal confinement based on pedestal measurements. Density scaling is positive for the core and negative for the pedestal:

$$\tau = 0.0148\, I^{0.8} n^{0.6} R^{2.2} P^{-0.6} M^{-0.2} + 0.29\, I^{2} R K^{2} M n^{-1} P^{-1}$$

The confinement data from shaping experiments normalised to this new scaling law are shown in Fig.13. The data now fit much better at high density with little systematic difference between data with different of elongation and triangularity.

Impurity seeding of the ELMy H-modes has been studied in a variety of conditions aimed at understanding the conditions allowing Radiation Improved (RI) modes to be accessed in JET. They include divertor L-modes at lower n/n_G fraction before the onset of sawteeth (more peaked density profiles), higher density L-modes limited on the outboard poloidal limiters and septum H-modes. RI modes are characterised by good confinement at densities well above the Greenwald limit resulting from peaked density profiles. Theory predicts a bifurcation when ion temperature gradient (ITG) fluctuations reduce before the emergence of trapped electron modes (TEM). Such a peaking of density has not been found, in line with theoretical analysis indicating that the domain for bifurcation remains inaccessible in most cases in JET. It is more accessible when more concentrated central particle sources and heavier impurity species are used. In effect, encouraging results have been obtained with H-modes sitting on the septum and using argon as a seed impurity [15]. A short delay after the gas puffing, an increase in the stored energy and of the density occurs, with a tendency to a peaking of the density profile. Carbon remains the main impurity in the core. In the afterpuff of septum H-modes, plasmas with good confinement at high-normalised density are thus achieved. In the database of the factor of merit: H_{97}x Greenwald density limit fraction shown in Fig.13**,** a figure of merit of 0.9 has been achieved at densities close to the Greenwald limit. With further optimisation, these techniques might be considered for application to ITER.

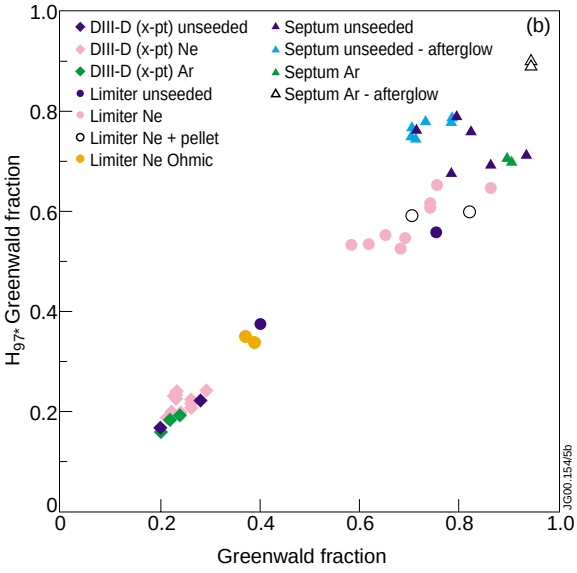

FIG.13. Data base for the H97xn_G fraction versus Greenwald fraction for the various scenarios developed to achieve RI modes.

3. Advanced Scenarios Studies

The aim of advanced scenarios is to produce plasmas with higher confinement and higher beta (both β_N and β_P) than the reference ITER ELMy H-mode. They are produced in JET with the so-called optimised shear scenarios [16] generating plasmas with internal transport barriers. The

latter are characterised by sharp discontinuities in the temperature and/or pressure profile gradients. Triggering of ITBs is very sensitive to the plasma current profile. Wide ITBs are usually produced when a low order rationale q surface is present within the plasma [17] and the foot of the ITB follows the radial evolution of the q =2 (or 3) surface which normally expands in time, thus producing wide barriers. Corresponding target magnetic shear values are low or close

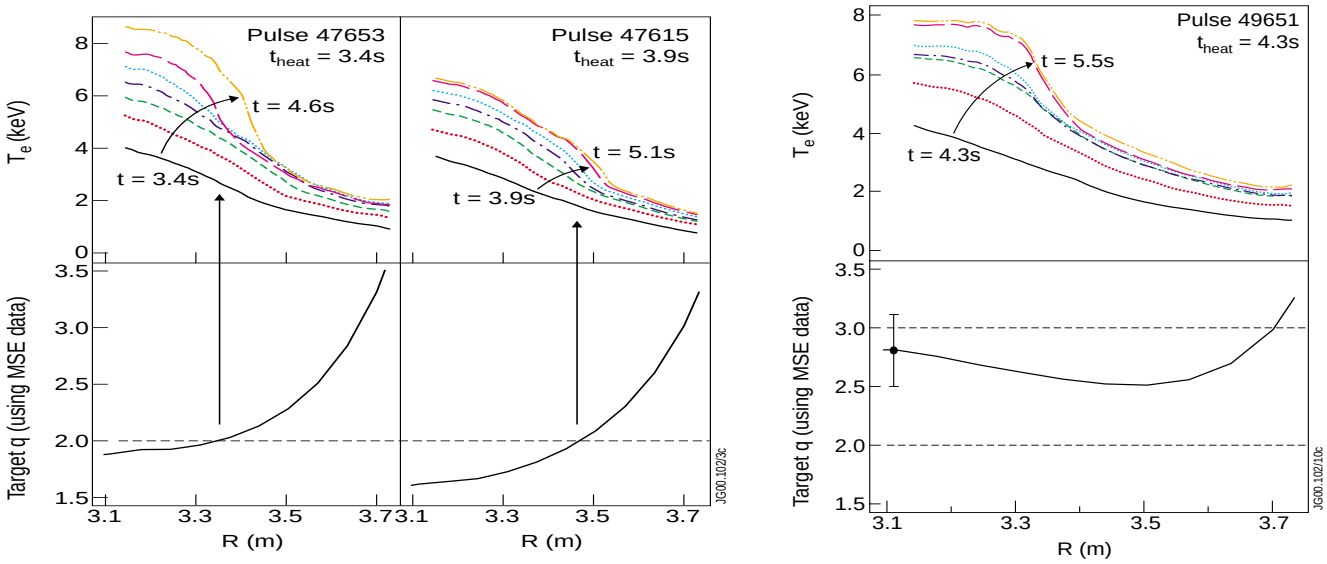

FIG.14. Evolution of ITBs (from ECE) for various magnetic shear target profiles (positive shear targest are produced with ICRH pre-heat, negative shear targets are produced with LHCD pre-heat)

to zero, but not negative (Fig.14). Application of Lower Hybrid Current Drive (LHCD) during the pre-heat phase allows negative values of the magnetic shear to be achieved with more internal ITBs that do not expand with time [18]. The two scenarios can co-exist producing multiple ITBs, increasing the flexibility of the scenario.

3.1 MHD stability

Most of the disruptions occurring during high performance plasmas with ITBs have been found to be due to n=1 kink modes and are well reproduced with ideal MHD codes [19], including some stabilisation effects from the wall. Disruptive stability limits have been found within 5% of calculated stability limits using the MISHKA code assuming a stabilising wall at 1.3 times the main plasma radius. These disruptions can be avoided by reducing the ion pressure peaking for operation at a given β_N [20]. As discussed in the following section, this can be achieved through operational techniques and non-disruptive plasmas with higher β_N can be produced close to the boundary limits. Other soft MHD events limit performance of ITB plasmas. Snakes [21] which are a double helix structure (m=2, n=1) can induce a local erosion of the ITB, which can eventually lead to large ELMs, and the subsequent destruction of the barrier. Snakes reside at or near the foot of the ITB with a radial extent of 5-10 cm, a poloidal extent of 30-60 cm and rotate at the local plasma frequency. Also, high n tearing modes (n up to 8) are routinely observed. They start from very small amplitude and increase locally the heat transport. Their neo classical nature has not been clearly established and as discussed later, they reduce confinement but are

not necessarily limiting β_N. The lower the ion peaking pressure, the less harmful are the MHD events.

3.2 ITB domain of existence

Developing scaling laws for the existence domain of ITBs, in view of defining the power needed on ITER to produce ITBs is an important issue. A strong dependence of the total injected power needed to generate an ITB with the magnetic field has been found as shown in Fig.15. It is interesting to note that the threshold power is reduced by a factor of 2 when LHCD is used in the pre-heat phase. Recent experiments indicate that this reduction is even more important at 3.4 T [22].

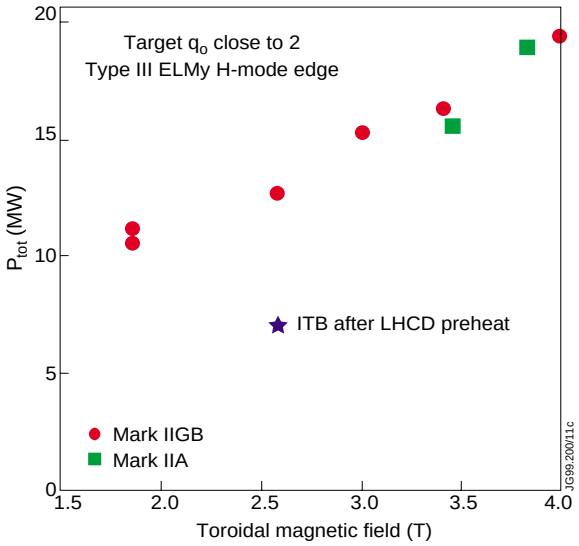

FIG.15. Total power (NBI + ICRH) needed to trigger an ITB as a function of the magnetic field for different scenarios.

Central heating is important to reduce the power threshold and the domain of ITB existence for different target current profiles is increased when the central power is increased. It has also been found that the power threshold is similar when NBI only or when equal NBI and ICRH power are used to trigger an ITB. The resulting ITBs are of similar quality and this shows that the initial torque is not a predominant effect. When equal ICRH and NBI power are used, ITBs are produced with similar ion and electron temperature profiles indicating that the improved confinement is not due to a hot ion effect. These facts are of interest for ITER since injected torque and central ion heating will be much reduced as compared to present experiments. A heuristic model which combines turbulence suppression or mitigation with combined ExB shear flow effects and of low or negative magnetic shear is being developed with some success [23] but a comprehensive parameter dependence model is not yet available.

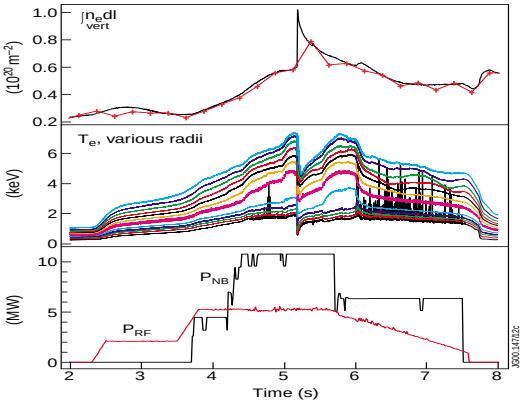

FIG.16. HFS pellet fuelling of an ITB. Te is given from ECE

3.3 Fuelling of ITBs

Fuelling the plasma core within an internal transport Barrier is an important issue for advanced scenarios since fuelling from NBI in ITER will be relatively low as compared to present experiments. Attempts have been made to use HFS and LFS pellet fuelling on ITB plasmas [7].

As shown in Fig.16, the confinement barrier is temporarily suppressed following a HFS pellet launch likely due to large changes in the plasmas edge. The ITB subsequently quickly recovers while the density decays but the time duration of the applied power was not long enough to possibly benefit from an increase in central density. These results are encouraging, but substantial optimisation remains to be done (time sequence, speed and size of pellets,) before this technique can be effectively used to fuel the ITB core.

3.4 High performances steady ITBs

Steady high performance ITB plasmas are achieved by controlling the plasma edge pressure with injection of noble gases, usually argon, with q_{95} close to 3 and high pumping at the edge [24]. This is in order to optimise plasma performance by operating at relatively high plasma current. With about 40% radiation, mainly from the edge, plasma current diffuses slightly faster and large steady q=2 surfaces can be established resulting in wide ITBs without too much peaking of the ion pressure. MHD problems such as n=1 tearing modes are thus avoided and deleterious effects induced by snakes are minimised. The MSE diagnostic indicates that the magnetic shear stays at slightly negative values. By carefully timing of the injected power waveform so to have a slow build-up of the pressure profile, steady plasmas with an efficiency factor $H_{89}x\beta_N$ in excess of 7

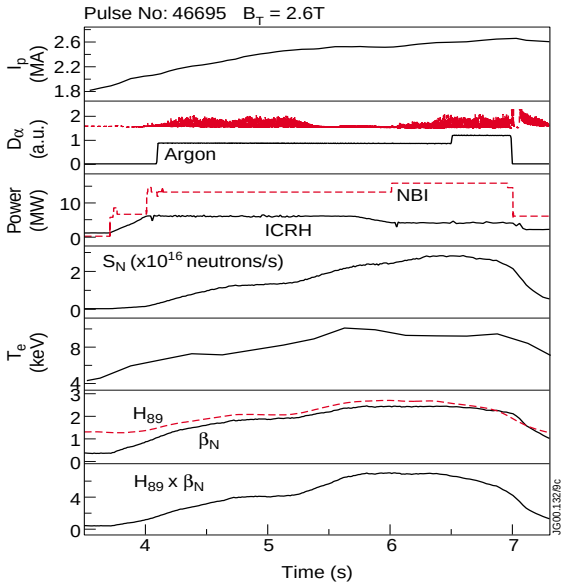

FIG.17 Time traces of typical signals of a steady high performance optimised shear plasmas at B=2.6T and Ip = 2.6 MA

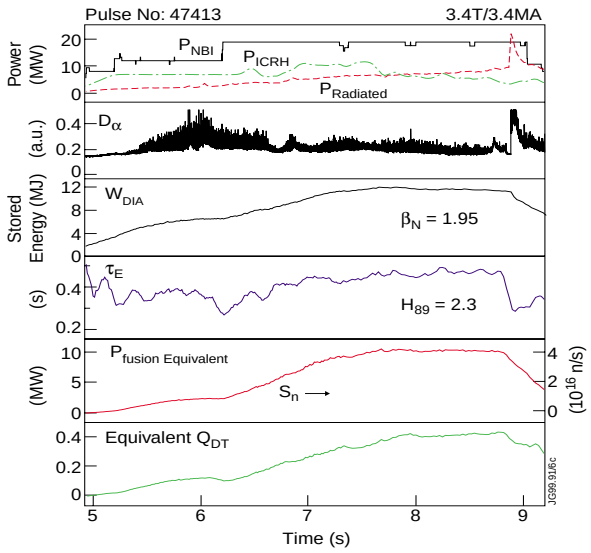

FIG.18.Steady high fusion yield achieved at B=3,4T and Ip=3.4MA with ITB plasmas and Argon edge control

can be obtained (Fig. 17). It is to be noted that the ELM activity with argon injection remains at a very low level. At a magnetic field of 3.4T, steady ITB plasmas with a DD neutron yield of $4x10^{16}$n/s have been maintained for several confinement times (Fig.18). The estimated equivalent fusion power in DT is 10 MW with an equivalent Q_{DT} of 0.4 [25]. The high performance phase can remain steady for as long as the additional heating power is applied but very often some events terminate prematurely the high yield phase by triggering an ELM free phase followed by a large type I ELM resulting in the subsequent destruction of the ITB. A

systematic study has indicated that the likely cause for these events is plasma interaction with the septum [26]. When the plasma beta is high enough while the strike points of the separatrix remain at the corner of the divertor plates in order to benefit from the highest pumping rate, plasma contact with the septum occurs (Fig.19). High pumping is needed in order to maintain the

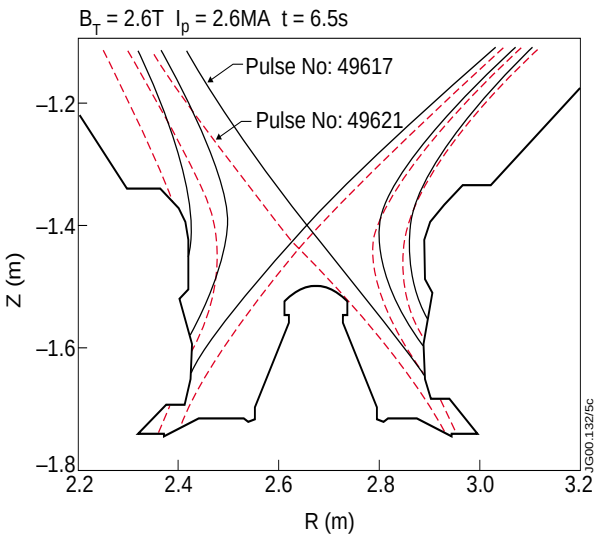

FIG.19. Last closed magnetic surfaces for pulse without (#49617) and with (#49621)septum avoidance technique allowing high beta pulse to be maintained.

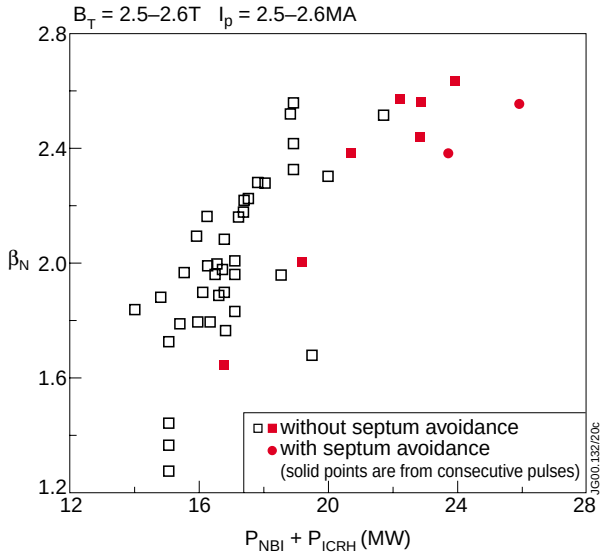

FIG.20. JET database for steady N versus total power at Bt~2.6T. Solid squares are for ITBs produced in consecutive pulses with similar scenarios. Solid circles are with septum avoidance techniques

edge parameters in the parameter space convenient for ITB formation (low density and high temperature at the edge [5]. Contact with the septum induces release of gas at the edge and the resulting change in the edge parameter space favours the production of ELM free plasmas. By moving the LCMS strike points on the divertor plates once the ITB is formed, septum interaction is avoided and steady β_N of 2.5 can be maintained for as long as the power is applied.

3.5 Beta limits and high β_P operation

An important issue for the assessment of the potentiality of advanced scenarios in ITER is to find at which beta it is possible to operate. As shown in Fig.20, the JET database for steady ITB plasmas at 2.6T **[**26,27**]** seems to indicate a saturation of β_N at a level of about 2.6. This database covers a large variety of scenarios. When consecutive pulses with an identical scenario are compared, saturation is not evident. In addition, data with the highest combined power (26 MW) were done with the septum avoidance technique resulting in slightly lower performance. A more definite answer on beta limits will be obtained when the septum is removed and when higher additional heating power becomes available. The database at 3.4T does not show indications of β_N saturation with the available power.

An attempt to produce plasmas directly relevant to ITER advanced scenarios with a high bootstrap current content and q_{95} in the range of 4 to 5 has been done. Good ITBs were produced for Bt=2.5T and Ip=1.5 MA in spite of significant ELM activity and some temporary collapses of the barrier. The difficulty was to produce plasma configurations with a high Shafranov shift that can also avoid an interaction with the septum. The remaining ELM activity indicates that this was not fully achieved. Good confinement plasmas (H_{89}=2.3) with β_N of 2.6 and β_P of 1.6 together with a significant neutron yield were produced [26]. A TRANSP analysis indicates that 60% of the current is non-inductively driven, the bootstrap fraction being 35% and the remaining non-inductive current being due to neutral beam current drive. Although a higher bootstrap current would be needed in ITER, a very encouraging feature is the fact that the total non-inductive current is rather well aligned with the total current as shown in Fig.21. This scenario can be substantially optimised, in particular following the removal of the septum.

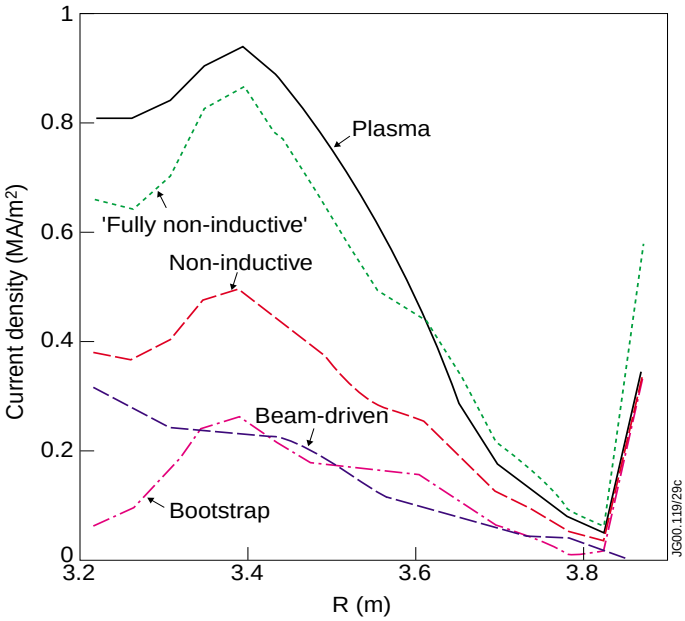

FIG.21. Radial profiles of various components of the plasma current from TRANSP analysis of pulse 49793 (Bt=2.5T, Ip=1.5MA). The dotted curve is an extrapolation of the total non-inductive assuming full current drive, thus showing the good alignment between total and non-inductive current drive

7. Summaries and conclusions

JET studies of the reference ITER ELMy H-mode have been instrumental for the definition of ITER-FEAT. The positive scalings of current and elongation which appears in the ITER 98 scaling law have been confirmed in a series of dedicated experiments. Increase of shaping of ITER-FEAT is therefore well supported. Confinement degradation at high density is attributed to a pedestal degradation. JET data fit better a two term model using respectively core confinement with a positive density scaling and edge confinement with a negative density scaling. MHD limit studies have focused on neo classical tearing modes. They show that ITER parameters are in the safer domain. Significant progress has been made in disentangling the role of various physics parameters but further work is required.

Using argon frost techniques, helium pumping and divertor enrichment have been found to be well within ITER requirements, therefore confirming in a large machine data already obtained on smaller devices. Target asymmetries and H-isotope retention, including tritium, are well simulated by modelling when taking into account drift flows in SOL and high sputtering factors. It has been found that a power of about 1.8 times the LH power threshold is required to maintain high confinement type I ELMs, a possible option for ITER. Fast particles do not seem to affect the edge.

Striking improvements in fuelling effectiveness has been found with the new high field side pellet launcher. Densities well above the Greenwald density limit have been achieved but with a degradation of confinement. By optimising the pellet sequence, it has been possible to maintain a good confinement at densities close to n_G. As well, Radiation Improved scenarios have been developed. Encouraging transient results have been obtained in the after-puff phase of septum H-modes.

Significant progress has been made developing integrated advanced scenarios with Internal Transport Barriers. Access domain studies have covered a wide domain including power threshold versus magnetic field and magnetic shear, comparison between ion heating and electron heating schemes, MHD boundaries for steady high beta operation and beta limits. Encouraging results for ITER have been produced: lower power threshold with negative shear (LHCD pre-heat) and influence of injected torque not predominant for ITB triggering (comparison ICRH/NBI). In spite of interesting modelling progress, a comprehensive scaling laws is still missing. MHD boundary limits have been explored identifying an operating domain where high beta ITB plasmas can be maintained for as long as the power is applied. The time duration of high β_N plasmas is limited by a plasma interaction with the septum. Beta limits cannot be properly assessed due to insufficient additional power and this septum interaction.

Integrated scenarios are in good progress by using edge impurity radiation control and pressure control. Steady fusion yield of 4 10^{16}n/s have been achieved, equivalent to ~ 10 MW in a 50% D-T mixture. Attempts to fuel an ITB with pellets have not yet been successful. This will require substantial optimisation. Plasmas with high β_N, high β_P and good confinement have been produced with 60% of the current being non-inductively driven with a good alignment with the total plasma current. Although a substantial development remains to be done, these results are very encouraging for application to ITER.

References

[1] MATTHEWS, G.F., et al., to appear in J. Nucl. Mater. (Proc. 14th Int. Conf. on Plasma Surface Interactions), paper O-4.2.

[2] CHANKIN, A.V., et al., to appear in J. Nucl. Mater. (Proc.14th Int. Conf. on Plasma Surface Interactions), paper I-4.1.

[3] COAD, J.P., et al., to appear in J. Nucl. Mater. (Proc. 14th Int. Conf. on Plasma Surface Interactions), paper I-2.1.

[4] STORK, D., et al., in Controlled Fusion and Plasma Physics (Proc. 26th Eur. Conf. Maastricht, 1999), Vol. 23J, European Physical Society, Geneva (1999) 205

[5] SARTORI, R., et al., in Controlled Fusion and Plasma Physics (Proc. 26th Eur.Conf. Maastricht, 1999), Vol. 23J, European Physical Society, Geneva (1999) 197

[6] The JET TEAM (prepared by RIMINI, F.), these proceedings, EX2/6

[7] JONES, T.T.C., et al., to appear in Controlled Fusion and and Plasma Physics (Proc. 27th Eur. Conf. Budapest, 2000), paper OR.004

[8] BAYLOR, L.R., et al, Nucl. Fusion **37** (1997) 445

[9] LANG, P.T., et al, to appear in Controlled Fusion and and Plasma Physics (Proc. 27th Eur. Conf. Budapest, 2000), paper P3.045

[10] SAIBENE, G., in "Descriptive Analysis of 1999 Task Force P data", JET Report

JET-R(00).
[11] BUTTERY, R., to appear in Cont. Fusion and Plasma Physics (Proc. 27th Eur.Conf. Budapest, 2000), paper T13.
[12] HENDER, T. et al, these proceedings (EXP3/02)
[13] The JET TEAM (prepared by MACDONALD, D.), these proceedings (EX2/3)
[14] HORTON, L.D., in Controlled Fusion and Plasma Physics (Proc. 26th Eur. Conf. Maastricht, 1999), Vol. 23J, European Physical Society, Geneva (1999)
[15] MADDISON, G.P., et al, these proceedings (EX5/4)
[16] THE JET TEAM (prepared by GORMEZANO, C.) Plasma Phys.and Cont.Nucl. Fusion Res., Proc.16th Int. Conf, Montreal, Vol I, IAEA Vienna, IAEA-CN-64/A5-5, (1996), 487
[17] SIPS, A.C.C., et al., Plasma Physics and Controlled Fusion 40 (1998), 1171-1184.
[18] CHALLIS C.D., et al., to appear in Cont. Fusion and and Plasma Phys.(Proc. 27th Eur. Conf. Budapest, 2000), paper OR.019
[19] HUYSMANS, G.T.A. et al., 24th EPS CCFPP, Berchtesgaden (1997) Vol. 1 (1997) 21-24.
[20] HENDER., in Controlled Fusion and Plasma Physics (Proc. 26th Eur. Conf. Maastricht, 1999), Vol. 23J, European Physical Society, Geneva (1999) 89-92.
[21] Alper, B., et al, in Controlled Fusion and Plasma Physics (Proc. 26th Eur. Conf. Maastricht, 1999), Vol. 23J, European Physical Society, Geneva (1999) 205
[22] THE JET TEAM, (prepared by PARAIL, V.V.), these proceedings (EXP5/05)
[23] PARAIL, V.V., et al., Nuclear Fusion 39 (1999) 429*;*
[24] THE JET TEAM (prepared by SIPS, A.C.C.), these proceedings (EX4/2)
[25] GORMEZANO, C., Plasma Phys. Control. Fusion **41** (1999) B367
[26] GORMEZANO, C., et al, to appear in Cont. Fusion and Plasma Physics (Proc. 27th Eur.Conf. Budapest, 2000), paper P1.048.
[27] THE JET TEAM, (prepared by BURATTI, P,) these proceedings (EX7/1)

Annex

THE JET TEAM

JET Joint Undertaking, Abingdon, Oxon, OX14 3EA, U.K.

J.M. Adams[1], P. Ageladarakis, B. Alper, H. Altmann, S. Arshad, N. Bainbridge, B.Balet, Y. Baranov[8], P. Barker, R. Barnsley[2], D.V. Bartlett, M.L. Begue[20], A.C. Bell, L. Bertalot[22], E. Bertolini, M. Beurskens[14], C. Bevil, A.J. Bickley, M. Bigi[22], S. Bird, K. Blackler, D. Bond, D. Borba[18] , M. Brandon, H. Brelen, P. Brennan, W.J. Brewerton, M. Brix[4], M.L. Browne, T. Budd, R. Budny[13], P. Butcher, R. Buttery[7], C. Caldwell-Nichols, D. Campling, P. Card, C.D. Challis, A.V. Chankin, M. Charlet, H. Chen, D. Chiron, J. Christiansen, D. Ciric, S. Clement, J.P. Coad, I. Coffey[7], S. Conroy[15], G. Conway, S. Cooper, J.G. Cordey, G. Corrigan, G. Cottrell, R. Cox, S.J. Cox, F. Crisanti[22], R. Cusack, N. Davies, S.J. Davies, J.J. Davis, R. de Angelis[22], P. de Antonis, M. deBaar[14], M. de Benedetti, N. Deliyanakis, A. Dines, S.L. Dmitrenko, J. Dobbing, N. Dolgetta, S.E. Dorling, H. Duquenoy, A.M. Edwards[7], C.G. Elsmore, J. Ellis, S.K. Erents[7], G. Ericsson[15], B. Esposito[22], H. Falter, J.W. Farthing, A. Fasoli[3], R. Felton, P. Ferrieres, J. Fessey, M. Fichtm ller, K. Fullard, M. Gadeberg, R. Garbil, A. Gibson, R.D. Gill, E. Giovannozzi[22], C. Giroud[20], D. Godden, J.K. Goff, A. Gondhalekar, A. Goodyear, C. Gormezano, C. Gowers, F.S. Griph, M. Groth[17], K. Guenther, H. Guo, A. Haigh, B. Haist[4] , D. Hamilton, C.J. Hancock, P.J. Harbour, J.D.W. Harling, N.C. Hawkes[7], N.P. Hawkes[1], D. Heading, R.F. Heeter[13], J.L. Hemmerich, O.N. Hemming, T. Hender[7], M. Hitchin, C.H.A. Hogben, L. Horton, J. Howie, M. Huart, C. Ingesson[14], J. Jacquinot, H. Jaeckel, J.F. Jaeger, O.N. Jarvis, J.P. Jeral, E. Joffrin[20], M. Johnson, E.M. Jones, T.T.C. Jones, J-F. Junger, C. Jupen[16], J. Kallne[15], A. Kaye, M. Keilhacker, N.G. Kidd, P. Knight[7], S. Knipe, A. Korotkov, P. Kupschus, R. LaHaye[9], P. Lamalle[23], J.R. Last, K. Lawson[7], M. Lennholm, C. Lescure, J. Lingertat, X.

Litaudon[20], P.J. Lomas, C. Lowry, R.M.A. Lucock, A.C. Maas[14], G. Maddison[7], P. Maget[20], C.F. Maggi, J. Mailloux, M. Mantsinen[5], J. Mart, D. Martin, G. Matthews, P. Mazon[20], G. McCracken, P.A. McCullen, D. McDonald, A. Meigs, R. Middleton, P. Miele, F. Milani, J. Mills, P. Morgan, F. Nave[18], G. Newbert, P. Nielsen, P. Noll, K. Norman, M. O Mullane, E. Oord, J. Orchard, V.V. Parail, A. Parkin, W. Parsons, B. Patel, A. Paynter, R.J.H. Pearce, A. Perevezentsev, M.A. Pick, J. Plancoulaine, S. Podda[22], O. Pogutse, R. Prentice, K. Purahoo, M. Rainford, J. Rapp[4], V. Riccardo, S. Richardson, F. Rimini, D. Robson, A. Rolfe, M. Romanelli, A.L. Roquemore[13], R.T. Ross, G. Saibene, F. Sartori, R. Sartori, Y. Sarazin[20], A. Schilham[14], P. Schild, M. Schmid, V. Schmidt, S. Sharapov, S.R. Shaw, A. Sibley, M. Simon, A.C.C. Sips, P. Smeulders, F. S ldner , J. Spence, R. Stafford-Allen, R. Stagg, M. Stamp, P. Stangeby[19], A.L. Stevens, D. Stork, P.E. Stott, J.D. Strachan[13], E.J. Strait[13], B.C. Stratton[13], P. Stubberfield, H.P. Summers[24], D. Summers, P. Svensson, M. Tabellini, J. Tait, T. Tala[6], A. Tanga, A. Taroni, D.S. Testa[3], P.R. Thomas, H. Thomsen[21], K. Thomsen, J.M. Todd, E. Traneus[15], A. Tuccillo[22], M. Tunklev, P. Twynam, M. von Hellermann, T. Wade, A. Walden, R. Walton, D. Ward, M.L. Watkins, N. Watkins[1], M.J. Watson, M.R. Wheatley, A. Whitehurst, C.H. Wilson, D. Wilson, H.R. Wilson[7], T. Winkel, D. Young, I.D. Young, K-D. Zastrow, M. Zerbini[22].

ADDRESSES

1. UKAEA, Harwell, Didcot, Oxon, UK.
2. University of Leicester, Leicester, UK.
3. Massachusetts Institute of Technology, USA.
4. KFA, Jülich, Germany.
5. Helsinki University of Technology, Espoo, Finland.
6. VTT Energy, Helsinki, Finland.
7. UKAEA Culham Laboratory, Abingdon, Oxon, UK.
8. A.F. Ioffe Institute, St. Petersburg, Russia.
9. General Atomics, San Diego, USA.
10. CRPP-EPFL, Lausanne, Switzerland.
11. Royal Institute of Technology, Stockholm, Sweden.
12. Imperial College, University of London, UK.
13. Princeton Plasma Physics Laboratory, Princeton, USA.
14. FOM Instituut voor Plasmafysica, Nieuwegein, The Netherlands.
15. Dept. of Neutron Research, Uppsala University, Sweden.
16. University of Lund, Sweden.
17. University of Manchester Institute of Science and Technology, Manchester, UK.
18. IST, Centro de Fuseo Nuclear, Lisbon, Portugal.
19. Institute for Aerospace Studies, University of Toronto, Canada.
20. CEA, Cadarache, France.
21. IPP Garching, Germany.
22. ENEA Frascati, Italy.
23. ERM, Belgium.
24. University of Strathclyde, Glasgow, UK.